Automated Design Architecture for Lunar Constellations

Article *in* IEEE Aerospace Conference Proceedings · December 2019

CITATIONS
3

READS
139

3 authors:

Ravi Teja Nallapu
The University of Arizona
45 PUBLICATIONS **160** CITATIONS
SEE PROFILE

Leonard Vance
The University of Arizona
15 PUBLICATIONS **27** CITATIONS
SEE PROFILE

Jekan Thangavelautham
The University of Arizona
205 PUBLICATIONS **828** CITATIONS
SEE PROFILE

Automated Design Architecture for Lunar Constellations

Ravi teja Nallapu
Space and Terrestrial Robotic Exploration (SpaceTREx) Laboratory
Dept. of Aerospace and Mechanical Engineering.
University of Arizona
Tucson, AZ 85721
rnallapu@email.arizona.edu

Leonard D. Vance
Space and Terrestrial Robotic Exploration (SpaceTREx) Laboratory
Dept. of Aerospace and Mechanical Engineering.
University of Arizona
Tucson, AZ 85721
ldvance@email.arizona.edu

Jekanthan Thangavelautham
Space and Terrestrial Robotic Exploration (SpaceTREx) Laboratory
Dept. of Aerospace and Mechanical Engineering.
University of Arizona
Tucson, AZ 85721
jekan@email.arizona.edu

Abstract— **Missions to the Moon are actively being developed for its scientific and engineering values. The Lunar Exploration Analysis Group (LEAG) has identified at least twenty enabling and enhancing goals to fulfill the existing lunar exploration Strategic Knowledge Gaps (SKG). Several of these goals will require multi-asset missions to the surface of the Moon involving human and machine interaction, as well as access to a ground station on Earth. Therefore, a communication enabling constellation deployed around the moon will serve as a crucial enabling technology for such missions. However, the limited orbital stability of lunar orbits constrains the use of traditional central body orbits for designing these constellations. The Earth-Moon Lagrange points, on the other hand, offer a viable location to deploy these constellations. The stationarity of the Lagrange points coupled with the fact that they have a large line of sight access area to the Moon's surface makes them a viable candidate for deploying constellations with a minimal number of spacecraft. However, the design of a Lagrange point constellation mission is not straight forward. This involves selecting the Lagrange points that offer the optimal coverage, optimal quasi-stationary trajectories around these Lagrange points, the optimal transfer to these trajectories, and the design of the constituent spacecraft. Clearly, this multi-disciplinary problem can benefit from a unifying mission design architecture that simultaneously handles the above-mentioned challenges. In our previous work, we developed the Integrated Design Engineering and Automation of Swarms (IDEAS) software do design swarm missions to solar system small bodies. This work will focus on extending the capability of the IDEAS architecture to design optimal constellations deployed at the Earth-Moon Lagrange points. The constellation will be designed to act as a relay network to Earth with a minimum number of spacecraft. The performance of the constellation will be noted by studying the accessible regions on the surface of the moon. The approach taken by this work is as follows. We begin by modeling the coverage of spacecraft antenna by studying the accessible areas. The spacecraft will be assumed to be in halo orbits about the colinear Lagrange points. A selection scheme for the halo orbits is then discussed in order to coverage, synchronization, and stability requirements. Finally, the principles described are demonstrated by designing a Lagrange point constellation with three spacecraft that have access to at least 85 % of the Moon's surface and can communicate with at least 70 % of the surface at any given instant. The requirements and performance of this constellation are then evaluated assuming state-of-the-art hardware capabilities. The results indicate successful performance of the developed algorithms thus enabling the IDEAS architecture to generate holistic optimal designs which will greatly increase the returns of the future missions to the Moon.**

TABLE OF CONTENTS

1. INTRODUCTION

Missions to the Moon offer significant science and engineering returns [1]. The Moon is also being considered as a viable platform for a human base [2,3]. The lunar exploration and analysis group (LEAG) has identified at least twenty enabling and enhancing goals to address to fulfill the exploration of the Moon [4]. These goals are broadly classified into three themes: *i.* study the lunar resources;

978-1-7821-2734-7/20/$31.00 ©2020 IEEE

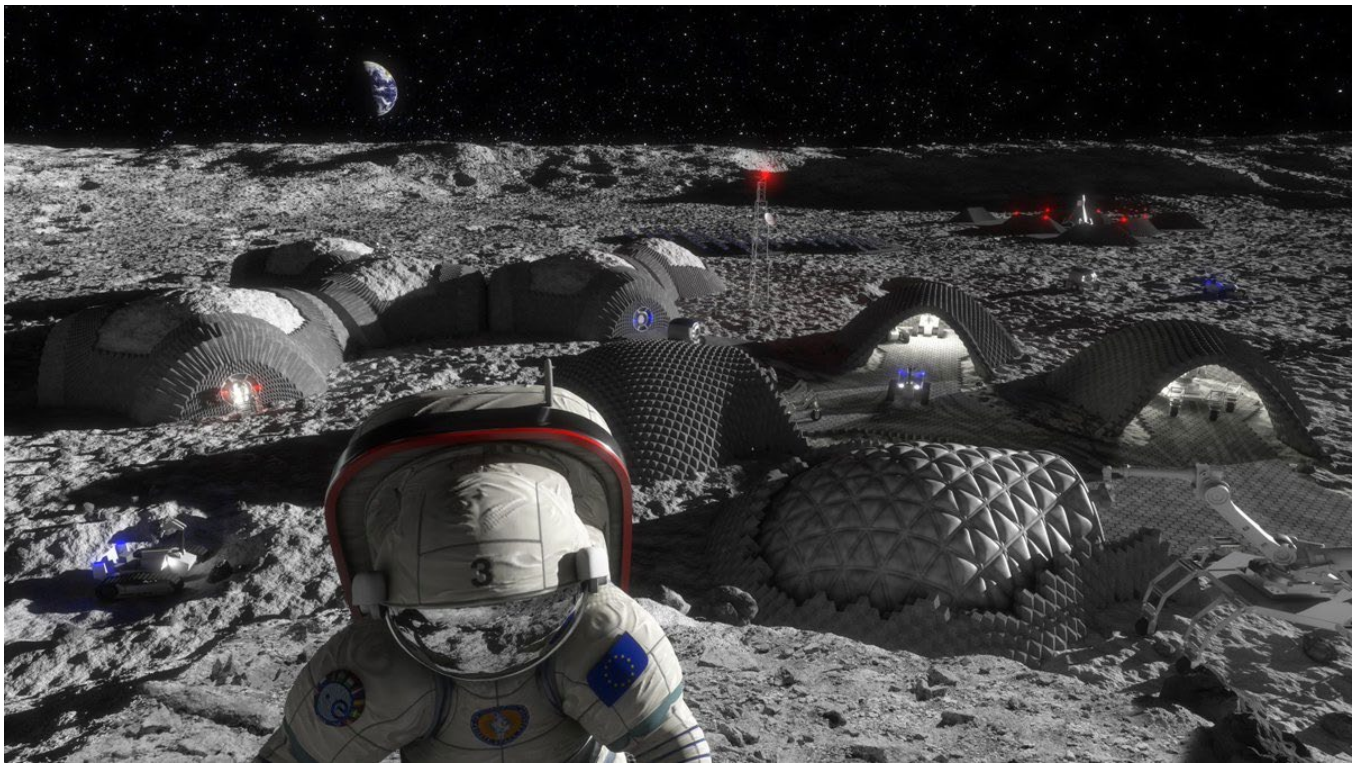

Figure 1. A conceptual Moon base highlighting different enabling technologies for human exploration of the Moon. (Image Source: Universe Today)

Strategic Knowledge Gaps (SKG) related to the human *ii*. study the effect of lunar environment on the lunar surface; and *iii*. enable working and living on the surface of the Moon. Since then several technological solutions and advances have been made to achieve these goals. Notable solution trends to these goals include design strategies for a lunar base [5, 6]; in situ excavation architectures [7, 8, 9], robotic solutions [10, 11, 12]; and development of life support systems [13, 14]. An artwork illustrating several of these challenges is shown in Figure 1. All such missions strongly rely on good communication architecture. Essentially, having a global communication architecture on the surface of the Moon increases the range of sites to deploy several of these missions. However, the Moon's surface is tidally locked resulting in permanently eclipsed regions that constrain global accessibility to its surface. One solution to enable a global communication architecture around the Moon is to deploy an orbiting spacecraft constellation. However, any constellation deployed in the immediate vicinity of the Moon faces two major issues. The beamwidth of communications spacecraft required to enable horizon to horizon coverage around the Moon is large, thus resulting in large constellation sizes and/or spacecraft in the constellations. Secondly, the instability of low Moon orbits constrains the accessibility of the constellation [15] and the constellation life [16]. The Lagrange points on the other hand offer potential solutions to deploy such constellations.

The current work presents a study on the design of a lunar constellation deployed at the Lagrange points using the IDEAS architecture. The Integrated Design Engineering and Automation of Swarms (IDEAS) architecture is an automated mission design software being developed to enable end-to-end interplanetary spacecraft swarm missions [17]. The IDEAS approach proceeds by dividing a swarm mission design into three individual design problems: trajectory design, spacecraft design, and swarm design. Once the individual design problems are identified, they are solved through automated architectures that employ evolutionary algorithms to search for optimal and holistic solutions. The current work will focus on designing a communication enabling constellation around the Moon deployed near the Lagrange points. Only the colinear Lunar Lagrange points (LL_1 and LL_2) identified through the circular restricted three-body problem [18] are used. The spacecraft will be deployed in Halo orbits near the Lagrange points. The optimal constellation will be a collection of northern and southern Halo orbits near LL_1 and LL_2 which satisfy the specified coverage, stability, and synchronization requirements.

We begin the current work by modeling the spatial and temporal coverage requirements of the constellation. In addition to these constraints on the halo orbits based on orbital stability and periods are presented, followed by developing a selection scheme for halo orbits based on these requirements. Evaluation of the constellation performance and requirements is also discussed. Finally, the algorithms discussed are demonstrated through numerical simulations. The organization of the current work is as follows: Section 2 presents relevant work done on lunar trajectories and constellations. Section 3 presents the methodology used in the current work. Here we formulate the constellation

requirements and the halo search scheme. The constellation design is then formulated as an optimization problem to minimize the number of spacecraft. Following this, we proceed to design an optimal lunar constellation in Section 4 which is able to meet the spatial and temporal coverage set by the mission designer. The performance of the optimal constellation is then studied. The implications of the current study followed by the contributions to the state of the art are discussed in Section 5. Finally, Section 6 presents a summary of the current work, and also identifies pathways forward, in order to facilitate IDEAS to design a communication enabling constellation around the Moon.

2. RELATED WORK

The dynamics of a spacecraft in the Earth-Moon system is a thoroughly studied problem in the literature. The circular restricted three-body problem (CR3BP) provides a good framework for designing spacecraft trajectories in the Earth-Moon system [19, 20]. The CR3BP entails five equilibrium points which, in the Earth-Moon system, are known as the lunar Lagrange points (LLPs) where a spacecraft would potentially come to rest. Three of these points (LL_1, LL_2 and LL_3) are located on the Earth-Moon line and are known as colinear points, while there other two points (LL_4 and LL_5) form equilateral triangles about Earth and the Moon (see Figure 3), and are known as the triangular points. In the current work, we will limit the design to the colinear Lagrange points alone. A major contribution to CR3BP was demonstrating the existence of a wide variety of periodic orbit families near the Lagrange points [20]. The halo family is a widely studied family of periodic orbits around the colinear points [21]. The halos are a family of non-planar periodic trajectories. The non-planar nature implies that they swing outside the Earth-Moon orbital plane and depending on where a large portion of their trajectories lie, they are classified into northern and southern halos. The southern halos are a reflection transformation of the northern halos about the orbital plane. Since accurate analytical solutions to these periodic motions are not known, numerical schemes to construct periodic families were developed [22, 23]. Several efficient strategies have been developed to construct these Halo orbits [24, 25]. Single shooting differential correction schemes are the most widely used numerical schemes for halo orbit construction. However, these schemes are sensitive to the first estimation of the initial conditions. Traditionally, analytical relations are used to provide the first estimate of initial conditions [26]. A thorough description of the state-of-the-art schemes to construct halo orbits, with applications to lunar schemes is provided by Grebrow et al [27]. Reference [27] also provides a catalog of initial guesses for several northern halos around the colinear points. Several guidance and control schemes have been proposed to deploy spacecraft in halo orbits [25, 28, 29]. An inherent challenge of halo orbits around the colinear points is their instability. Due to this reason, much research has focused on station keeping on these orbits [30, 31]. The applications of deploying spacecraft in halo orbits are also wells studied in the literature. Farquhar studied the coverage of a spacecraft in a halo about LL_2 to provide uninterrupted access to the far side of the Moon [32]. Ely et al designed constellations deployed on frozen orbits to provide global coverage of the Moon [33]. Multi-halo constellations, and communication enabling halo orbit constellations have also been designed [34, 35].

Traditionally, multi-spacecraft missions are designed based on decoupled design architectures with each component of the mission is designed separately [36]. The challenge with these approaches is that individually optimal designs might not be holistic and would often require several iterations to converge to a feasible optimal design. Therefore, a unifying mission design architecture would lead to holistically optimal designs that can provide a better quality of swarm missions. To address these challenges, we developed IDEAS as an end-to-end mission design architecture to design interplanetary spacecraft swarm missions [17]. In Reference [17] we also presented a spacecraft coverage evaluation algorithm when the spacecraft has a generic square sensor, and the target body is a distribution of cartesian coordinates. We then introduced a new classification of spacecraft swarms [37] which encompasses a wide range of architectures ranging from constellations to formation flying swarms. Such a classification allows us to define a unifying scheme for defining swarm architectures. We classified swarms into five classes as follows:

Class 0 Swarms. A Class 0 swarm is a collection of multiple spacecraft that exhibit no coordination either in movement, sensing, or communication.

Class 1 Swarms. In a Class 1 swarm, the spacecraft coordinate their movement resulting in formation flying but there is no explicit communication coordination or sensing coordination.

Class 2 Swarms. In a Class 2 swarm, the spacecraft coordinate movement and some amount of communication through MIMO or parallel channels. Has sensing but is not optimized to swarm or is post-processed.

Class 3 Swarms. A Class 3 swarm coordinates sensing/perception with communication and positioning/movement but doesn't fully exploit the three concurrently. Individual losses can have uneven outcomes include total loss of the system.

Class 4 Swarms. Finally, a Class 4 swarm exploits concurrent coordination of positioning/movement, communication and sensing to perform system-level optimization. The system acts if it's a single entity, computing between entity is distributed. Individual losses result in a gradual loss in system performance.

Using these architectures, we demonstrated the capability of IDEAS to design Class 1 [17] and 2 [37, 38] swarms to explore small bodies. We also applied the IDEAS framework to design a Class 0 swarm for monitoring meteor events [39]. The current work will focus on designing a constellation (Class 0 swarm) deployed near LL_1 and LL_2, in order to

enable global communications access to the surface of the Moon.

3. METHODOLOGY

This section describes the methodology of the current work. We begin by describing the coverage requirements of the constellation. We then describe the dynamics of halo orbits and their design constraints. Next, we pose the constellation design problem as a minimization problem. We then present the relations to evaluate the performance of the communications constellation, if it were realized using small satellite grade transceivers.

Surface coverage

Consider a spacecraft in the constellation which orients its transmitter towards the Moon as shown in Figure 2. The radius of the Moon is denoted by R_M and the position vector from the spacecraft to the Moon is denoted by $\bar{r}_{SM}$. When oriented towards the Moon, the transmitted has access to the entire surface that spans the horizon. However, to prevent limb losses, the minimum elevation angle ε_O can be specified as a factor of safety.

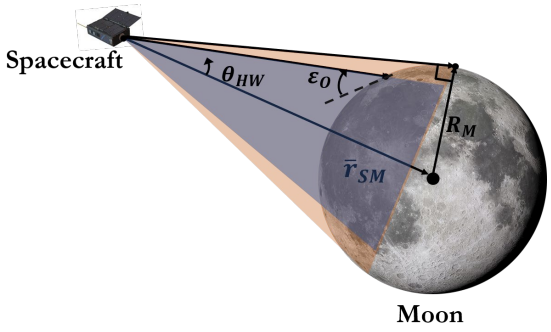

Figure 2. Setup of the coverage evaluation problem showing the horizon-horizon beamwidth (orange), and the required beamwidth (blue).

The required half beamwidth θ_{HW}, subtended by the Moon's surface for a minimum elevation angle ε_O can be calculated from spherical geometry as:

$$\sin\theta_{HW} = \frac{R_M}{|\bar{r}_{SM}|}\cos\varepsilon_O \tag{1}$$

The shape of the Moon is described by a distribution of cartesian vertices V_M, and a set of triangular faces F_M describing the vertex connectivity. The objective of the coverage problem is then to determine the surface area of the faces of the shape model, that falls inside the transmitter's beamwidth at a given instant. Once, the set of faces observable by spacecraft-j at time t, $(F_j(t) \subseteq F_M)$, are determined, the area observed by this spacecraft at this time $A_j(t)$ can be obtained by adding the areas of the triangles described by these faces. This area can now be expressed as a percentage of the total surface of the Moon as:

$$P_j(t) = \frac{A_j(t)}{A_M} \times 100 \tag{2}$$

Where, A_M is the surface area evaluated using all the faces of the shape model. Our previous work [17] presented coverage evaluation algorithms to evaluate the coverage of a generic sensor. The algorithm has two operations on the point cloud model: culling and clipping. Culling eliminates vertices that are eclipsed by the surface, while clipping is a linear transformation that eliminates vertices that lie outside the sensor's specified field of view. It needs to be noted here that the algorithm was developed for evaluating the visual coverage of a pin-hole camera. In the current work, the same algorithm is used while generalizing the sensor to a communications transmitter. In the current work, a 12 k triangular face model is used to model the surface of the Moon [40]. Due to the dynamical nature of the problem, several figures of merit (FoM) are possible. Two FoM are used in the current work to evaluate the coverage of a swarm containing N_{sw} spacecraft.

Total instantaneous coverage—This metric describes the total area observed by the constellation at a given time instant. If the faces observed by the individual spacecraft at a given time are known, the faces observed by the constellation at that instant $F_C(t)$ is obtained by performing a set union operation of the observable faces, i.e.,

$$F_C(t) = \bigcup_{j=1}^{N_{sw}} F_j(t) \tag{3}$$

Global orbital coverage—This metric describes the total area cumulatively observed by the constellation during one orbital period of a spacecraft in the constellation. While, it is completely possible that all spacecraft orbits, will not have the same orbital period, we take the minimum orbital period T_{min} to evaluate the cumulative coverage of the constellation. The set of faces used for computing the global orbital coverage are given by

$$F_G = \bigcup_{t=0}^{T_{min}} F_C(t) \tag{4}$$

Equation 2 is used to compute the percentage of instant coverage $P_C(t)$ and percentage of global orbital coverage P_G using Equations 3 and 4 respectively.

Spacecraft dynamics

As described earlier, halo orbits are periodic orbits near the colinear Lagrange points described by the CR3BP. The CR3BP is typically set up in a canonical Barycentric frame, where the x axis connects the center of the primary mass (Earth) to the secondary mass (Moon). The z axis is along the upward normal to the orbital plane of the secondary.

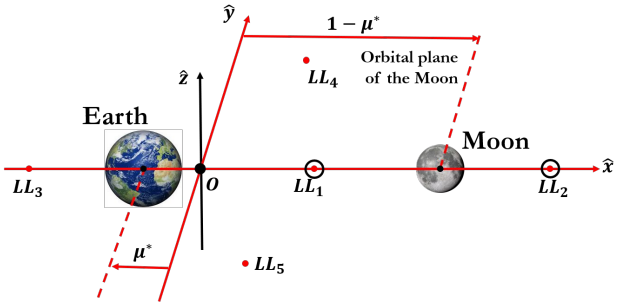

Figure 3. The canonical barycentric frame used for the defining the Earth-Moon CR3BP.

The origin is located at the center of mass of the Earth and the Moon. The system is scaled so that the Earth-Moon distance and the angular velocity of the Moon are normalized to unity. This results in a scaled distance unit (DU) of 1 DU = 384400 km, and a scaled time unit TU of 1 TU = 4.34 days. The distances are parameterized by a dimensionless mass fraction μ^* of the Moon given by:

$$\mu^* = \frac{M_M}{M_M + M_E} \tag{5}$$

Where, M_M and M_E denote the masses of Moon and the Earth respectively. As expected, this is a rotating frame, where the x axis rotates with the orbital position of the Moon. The spacecraft motion in the barycentric frame is obtained by propagating the Cartesian equations of motion. In addition to this, the state transition matrix (STM) is also, which linearly maps the initial state to the state at a time t_f, denoted by $\Phi(0, t_f)$, is also propagated [24].

Halo orbit design

In the current work, we use a single shooting differential strategy to construct the halo orbits of the spacecraft. The construction involves guessing an initial condition $\bar{r}'_s(0)$, and a time period T'_P. The initial guess for $\bar{r}'_s(0)$ is commonly expressed in the format

$$\bar{r}'_s(0) = [x'_0 \quad 0 \quad z'_0 \quad 0 \quad v'_{y0} \quad 0]^T \tag{6}$$

The dynamics of the spacecraft and the corresponding STM are propagated to half the estimated orbital period $T'_P/2$. Based on the values of the x and z component velocities at $T'_P/2$, the values of z_0, v_{y0} and T'_P are corrected using the STM. The scheme then proceeds iteratively by adjusting the control variables to drive the x and z component velocities at $T'_P/2$ to 0. Due to numerical reasons, the scheme is usually cut off by specifying a tolerance ε_{DC} and the maximum number of iterations N_{DC}. If the tolerance constrained is satisfied, the corrected initial conditions denoted by

$$\bar{r}^*_s(0) = [x'_0 \quad 0 \quad z^*_0 \quad 0 \quad v^*_{y0} \quad 0]^T \tag{7}$$

and the corrected time period denoted by T^*_P specify a halo orbit. Following this, the trajectory of the spacecraft starting from $\bar{r}^*_s(0)$ is then propagated for the corrected time period T^*_P. The STM obtained at the end of T^*_P is called the monodromy matrix Φ_M, and is useful for describing orbital stability.

Stability—The monodromy matrix is characterized by six eigenvalues which form three reciprocal pairs, i.e., an eigenvalue pair of the monodromy matrix is expressed as $\left(\lambda_i, \frac{1}{\lambda_i}\right)$. Thus, the monodromy matrix is characterized by three independent eigenvalues. Additionally, one of these independent eigenvalues has unit magnitude. The other two eigenvalues are used to describe the stability of the halo orbit. The stability is usually specified by a stability index ν which indicates the time constant for the spacecraft to exit the halo orbit. The stability index of the halo orbit is defined as:

$$\nu = \frac{1}{2}\max\left(\left|\lambda_i + \frac{1}{\lambda_i}\right|\right) \tag{8}$$

The orbits with stability index $\nu = 1$ represent highly stable orbits, where the station-keeping fuel requirements are minimum. The stability decreases as ν exceeds unity thus requiring higher stability. An observed trend is that as ν is maximum for halo orbits in the vicinity of the parent Lagrange point. Additionally, as ν approaches unity, we start finding halo orbits near the Moon.

The constraint on the constellation that the stability index raises is that highly stable orbits are near the Moon which requires a large number of spacecraft in the constellation due to the high beamwidth described by Equation 1. Orbits with a large ν, have low beamwidth requirement but have stricter station-keeping requirements. Therefore, a stability constraint can be placed on the constellation which requires the maximum stability of the constellation ν_{max} to be below a required parameter ν_r.

Period synchronization—As described above, the numerical specification of the halo orbits will result in constellations where all spacecraft have different orbital periods. Large discrepancies in orbital periods will result in gaps in surface coverage. Therefore, a synchronization constraint is placed which requires that the difference between the maximum and minimum orbital periods of spacecraft in the constellation be below a specified tolerance, ε_T.

Halo directions—The halo orbits are further classified as north and south depending on the region which contains a large portion of their out of plane trajectory. Northern halos have a large z amplitude in the $+z$ direction, while the southern halos have a large z amplitude in the $-z$ direction. The southern halos can be constructed with the same information given to construct the northern halos, through a reflection transformation about the $x-y$ plane as seen in Figure 4. If $[x'_0 \quad 0 \quad z'_0 \quad 0 \quad v'_{y0} \quad 0]^T$ describes the initial guess for a northern halo with an estimated time period T'_P, the reflected state $[x'_0 \quad 0 \quad -z'_0 \quad 0 \quad v'_{y0} \quad 0]^T$ is the initial guess for a southern halo for the same time period.

Initial conditions—While the initial guesses for the parameters x'_0, z'_0, v'_{y0} and T'_P are typically obtained from a Richardson-Cary analytical approximation, the current work uses a catalog of initial conditions to search for the optimal halo orbits. Grebrow et al. [26] provides a distribution of the initial conditions required to produce northern halo orbits around LL_1 and LL_2. The distribution of the initial guess parameters and their estimated stability indices used in the current work are shown in Figure 4, as a function of the x axis offset, which is given by

$$\Delta x = x'_0 - x_{LL_i} \tag{9}$$

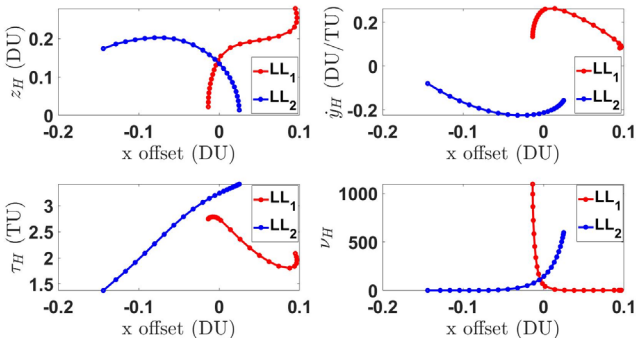

Figure 4. The distribution of initial conditions used in the current work used to construct northern halo orbits near LL_1 and LL_2.

Where, x_{LL_i} is the x coordinate of the Lagrange point i. Each data point shown in Figure 4 is given an integer designation which will specify the corresponding halo orbit. The distribution for the southern halo orbits is produced by the reflection operation described above. It should be made explicit here that while the northern halo distribution is used to generate the initial conditions for the southern halo orbits, specifying one orbit in the reflected pair does not necessarily mean that the other is used. This is also illustrated in Figure 5, where the constellation has a reflected halo pair at LL_1, but the halos at LL_2 are not reflections of each other.

Constellation Design—In order to achieve global coverage of the Moon, the spacecraft in the constellation are deployed in a combination of north and south halos near LL_1, and LL_2. An illustration of a sample constellation is presented in Figure 4. If a constellation has spacecraft in $N_{L,i}$ northern halo orbits and $S_{L,i}$ southern halo orbits near Lagrange point i, the constellation size is given by

$$N_{sw} = \sum_{i=1}^{2} (N_{L,i} + S_{L,i}) \tag{10}$$

In this work, we are interested in designing a constellation with a minimum number of spacecraft, which satisfies the coverage, stability, and period requirements described above.

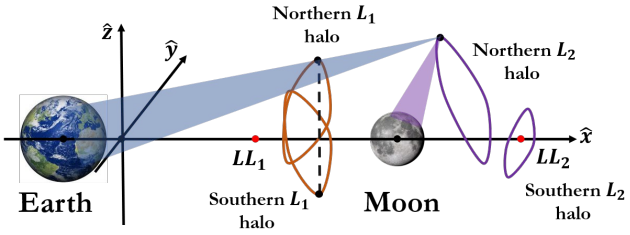

Figure 5. An example of four spacecraft constellation containing a combination of northern and southern halo orbits near LL_1 and LL_2.

The optimal constellation design problem is now expressed as

$$\min N_{sw} \tag{11}$$

such that

$$P_G \geq P_{R1}$$

$$P_C(t) \geq P_{R2} \quad \text{when } t \leq T_{min}$$

$$v_{max} \leq v_r$$

$$T_{max} - T_{min} \leq \varepsilon_T$$

The design variables for the optimization problem in Equation 11 are presented in Figure 6.

Communication performance

Once the constellation is designed, we would be interested in the implications that the design has on the spacecraft, and also on the communication performance. The objective of the constellation is to act as a global relay station between the Moon and the Earth. One configuration to achieve this is to design each spacecraft in the constellation with two communication systems. One system would transmit data to the surface of the Moon. The other would transmit data back to Earth as seen in Figure 5. Of specific interest, are the antenna sizes required for the transmissions, and the data transfer rates enabled at a ground station on Earth. This section presents the relations required to analyze the link budget and antenna sizing of the constellation.

Antenna performance—Selection of a communications subsystem implies that its broadcast frequency f_s, and transmission power P_{Tx}. The communications system will have to transmit its power through a directional beam whose full beamwidth θ_{BW} computed using Equation 1. Note that Equation 1 provides the half beamwidth angle θ_{HW}. The aperture diameter D_A of the antenna is given determined from θ_{BW} through the following empirical relation [36]:

$$D_A = \frac{21}{f_s \theta_{BW}} \tag{12}$$

Parameter	$\#LL_1$ northern halos	$\#LL_1$ southern halos	$\#LL_2$ northern halos	$\#LL_2$ southern halos	$N_{L,1}$ indices	$S_{L,1}$ indices	$N_{L,2}$ indices	$S_{L,2}$ indices
Variable	$N_{L,1}$	$S_{L,1}$	$N_{L,2}$	$S_{L,2}$	$j_1 \mid j_2 \mid \cdots \mid j_{N_{L,1}}$	$j_1 \mid j_2 \mid \cdots \mid j_{S_{L,1}}$	$j_1 \mid j_2 \mid \cdots \mid j_{N_{L,2}}$	$j_1 \mid j_2 \mid \cdots \mid j_{S_{L,2}}$
Range	Integer $[0, N_{max}]$	Integer $[0, N_{max}]$	Integer $[0, N_{max}]$	Integer $[0, N_{max}]$	Integer $[1, N_{1,max}]$	Integer $[1, N_{1,max}]$	Integer $[1, N_{2,max}]$	Integer $[1, N_{2,max}]$

Figure 6. Gene map of the design variables used in determining the optimal halo orbit constellation.

Where, D_A is expressed in m, f_s is in Hz , and θ_{BW} is in deg. The aperture diameter is useful in determining the transmitter gain G_{Tx} given by

$$G_{Tx} = \eta_A \left(\pi D_A \frac{f_s}{c}\right)^2 \tag{13}$$

Where, η_A is the antenna efficiency, and c is the speed of light.

Ground station—The data received at the ground station is a crucial performance indicator of a communications mission. Let us assume that the ground station has a receiver with gain G_{Rx}, a noise temperature level T_s, and is located at a distance r_{gs} from the spacecraft. The power received at the ground station is given by

$$P_{Rx} = \frac{P_{Tx} G_{Rx} G_{Tx}}{\left(4\pi r_{gs} \frac{f_s}{c}\right)^2} \tag{14}$$

The data rate of reception R of this input power corresponding to a bitrate error requirement of B_{ER} is given by

$$R = \frac{P_{Rx}}{kT_s \left(\frac{E_b}{N_o}\right)} \sin^2 \beta \tag{15}$$

Where, k is the Boltzmann's constant, β is the phase modulation index, and $\frac{E_b}{N_o}$ is the signal to noise ratio, which is computed from the bitrate error requirement as

$$\frac{E_b}{N_o} = \left(\text{erfc}^{-1}(2B_{ER})\right)^2 \tag{16}$$

The relations described in Equations 12-16 depend on the beamwidth and distance to the ground station. Since the beamwidths and relative distances to Earth change dynamically in the mission, we note the maximum beamwidth, and a maximum distance of the spacecraft in the constellation to estimate the performance. Strictly speaking, the maximum beamwidth will be coupled with the minimum range through Equation 1, however noting the parameters separately will be useful in providing conservative estimates. The performance of the constellation is summarized in Figure 7. We now proceed to design an optimal constellation, followed by analyzing its performance.

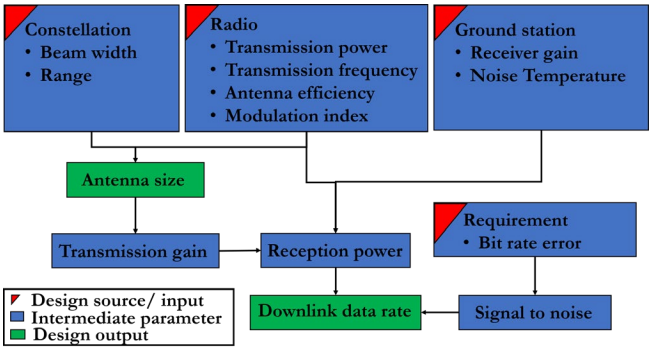

Figure 7. Requirement flow diagram showing how the design parameters influence the communication performance.

4. RESULTS

This section applies the principles described above, to design a constellation that global orbital coverage of at least 85 % at a total instantaneous coverage of at least 70 % at any given time. We begin by discussing the results of optimization and follow this with an analysis of the constellation performance.

Optimization

The optimal constellation is designed by solving the minimization problem described in Equation 11. A mixed-integer genetic algorithm solver [41] is used to solve the constellation design problem. The parameters input to the optimizer are presented in Table 1.

The optimization algorithms explored around 40 generations of designs during each run. Each generation evaluated 40 individual genes. The optimizer runs typically converged to an optimal solution in around 18 generations to design with constellation size of $N_{sw} = 3$ spacecraft. The problem was solved five times to verify the convergence of the solution. The evolution of the mean and best designs in a generation was recorded during each run. The distribution of mean and best designs captured from the multiple optimizer runs are presented in Figure 8.

Constellation design

The optimal constellation resulted in a 3 spacecraft constellation with an LL_1 north (NLL_1), LL_1 south (SLL_1), and LL_2 south (NLL_2), orbits as shown in Figure 9. The key characteristics of the constellation are summarized in Table 2. As seen in Table 2, the designed constellation has a maximum stability index of 457. Additionally, the maximum

Table 1. Input parameters to the constellation optimization problem

Parameter	Value
P_{R1}	85 %
P_{R2}	70 %
v_r	1000
ε_T	2 hrs
ε_O	30 deg
N_{max}	5
$N_{1,max}$	20
$N_{2,max}$	20
ε_{DC}	10^{-13}
N_{DC}	100

and minimum orbital periods are found to differ by about 1 hr as seen here. This suggests that the designed constellation is indeed able to meet the stability and period synchronization requirements.

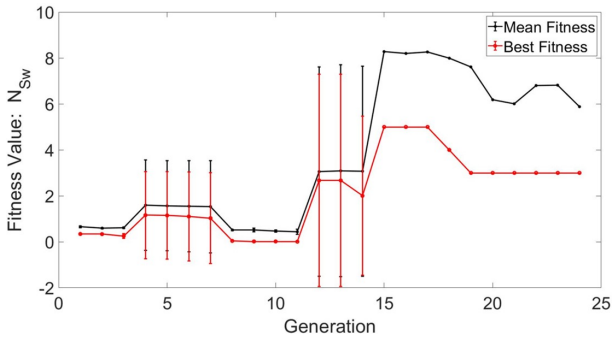

Figure 8. Evolution of the mean and best designs noted through multiple runs of the optimizer.

Table 2. Characteristics of the spacecraft in the optimal constellation.

Parameter	Orbit 1	Orbit 2	Orbit 3
Halo type	NLL_1	SLL_1	SLL_2
z amplitude (km)	45518	31675	74432
Period (days)	**12.1 (291 hr)**	**12 (290 hr)**	12.1 (290 hr)
Stability index	170	**457**	12.1

Coverage performance—The coverage performance of the constellation during their operation is presented in Figure 10. As seen here individual spacecraft in the constellation have access to about 33 % of the surface. The total instantaneous coverage varies between $70 - 78$ % of the surface during the 12 hr orbital operation. During this period, the constellation has cumulative access to the complete surface as shown in Figure 11.

Communication performance

In order to study the performance of the constellation, we assume that the spacecraft has a CubeSat grade transceiver. The JPL Iris radio is assumed as the communications subsystem [42]. The deep space network (DSN) is used as a baseline to calculate the data rates on the ground [43]. A conservative bite error rate of $BER = 10^{-6}$ is used as the requirement to estimate the data rate at Earth. The parameters used to analyze the performance of the constellation are presented in Table 3. In addition to these, the maximum beamwidths, and maximum distances of the spacecraft to Earth and the Moon are noted by propagating the trajectories of the spacecraft. In the case of the transmitting data down to Earth, the size of the antenna required, along with the transmission data rates is calculated.

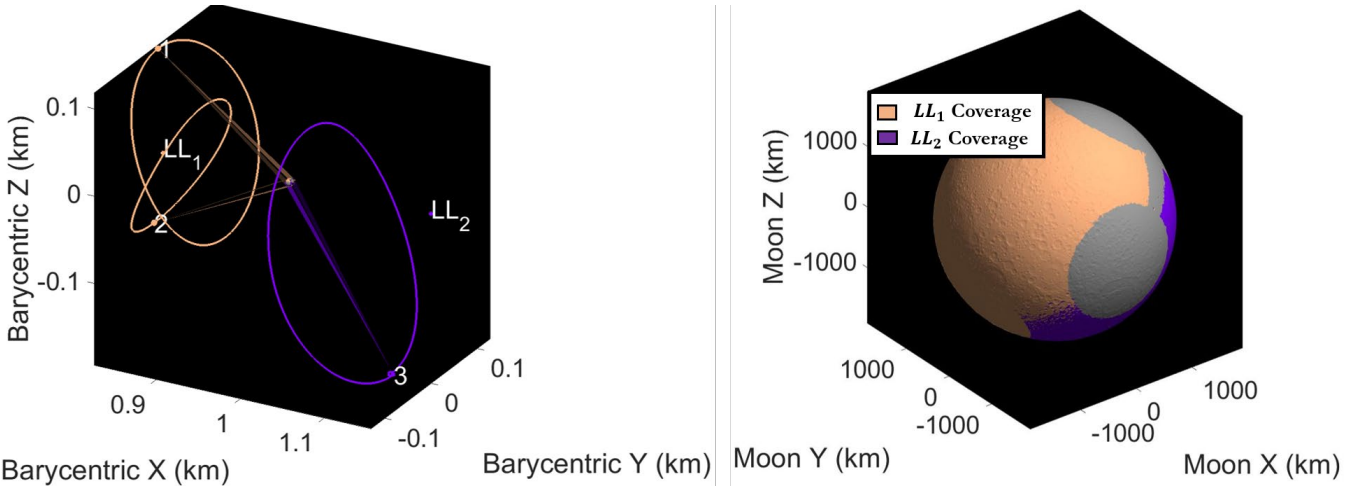

Figure 9. The optimal three spacecraft halo orbit constellation (left), and their total instantaneous ground coverage pattern at the sampled instant (right).

Table 3. Parameters corresponding to the transmitter, and requirements used to estimate the constellation performance.

Parameter	Value
Transmission power	4.8 W
Transmission Frequency	8.4 Hz
Antenna efficiency	55 %
Phase modulation index	60 deg
Receiver gain	68.2 dB
Noise temperature	29.2 K
Bit error rate	10^{-6}

In case of the transmissions to the Moon the size of the antenna required for the transmission alone is computed. The results of these computations are presented in Table 4.

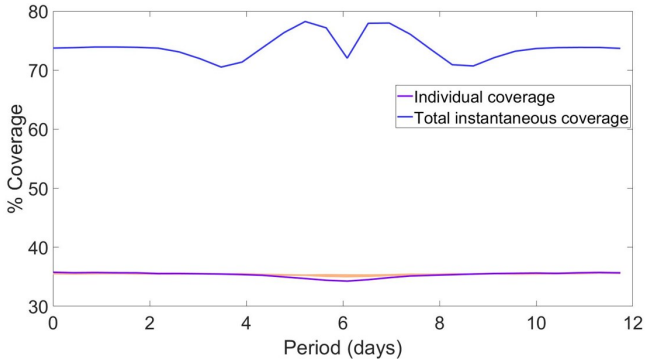

Figure 10. Temporal coverage of the constellation, showing the accessible area by individual spacecraft, and total instantaneous coverage area.

As seen in Table 1, the communication systems require moderately sized antennas: about 1.1 m and 0.32 m for the Earth and the Moon respectively. This is indeed achievable by state-of-the-art small spacecraft technology. In addition to this, the constellation will be able to transmit data to Earth at a rate of 1.14 $Gbps$.

5. DISCUSSION

The current work addresses some important aspects of designing a relay constellation around the Moon. The first is the multidisciplinary aspect of the problem. The current work used dynamical and coverage constraints to obtain optimal constellation. Additional constraints such as station-keeping requirements, halo insertion fuel, can be used to provide more practical solutions. Next, typical halo orbit studies focus on the spacecraft dynamics alone, which can result in designs that are dynamically optimal but may not be practical. These problems are even challenging in the case of designing swarm missions. Furthermore, while in the current work we fixed the communication radio in order to analyze the constellation performance. However, in a real mission, these can turn out

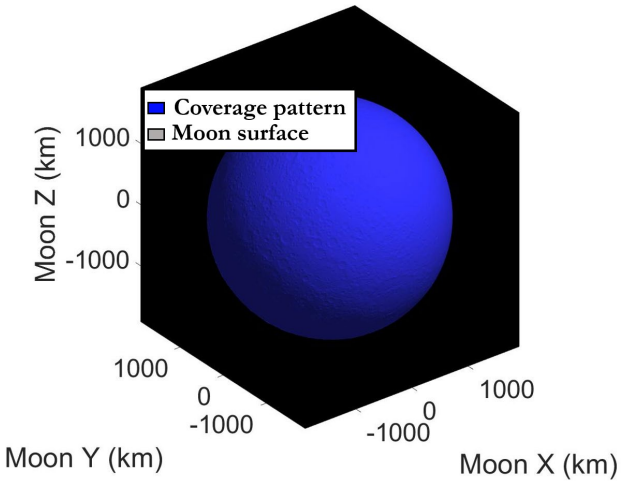

Figure 11. Global orbital coverage of the constellation. The constellation has access to the complete surface during one orbital period.

to be constraints or variables. Thus, having a unifying automated architecture such as IDEAS can result in both optimal and practical designs that are otherwise unintuitive to a human mission designer. The current work has three important contributions to the state-of-the-art mission design architectures. First, in the current work, we presented a unifying architecture to design halo orbit relay constellation around the Moon. Next, we presented coverage evaluation algorithms to study the dynamical coverage of these halo constellations. Finally, using the algorithms presented, we designed an optimal three spacecraft constellation in halo orbits near the LL_1 and LL_2 points. A preliminary analysis was also developed on the practicality of the constellation, which suggested that using CubeSat grade X-band transceivers, the constellation is able to provide downlink data rates greater than 1.14 bps when interfaced with the DSN.

6. CONCLUSION

The current work presented a new mission design architecture to design a relay constellation around the Moon. The constellation would be deployed in halo orbits near the colinear lunar Lagrange points LL_1 and LL_2. We developed the coverage evaluation algorithms for the constellation to evaluate instantaneous and global coverage of the Moon. Additionally, we also developed constraints based on orbital stability and synchronization. These constraints are then used to select an optimal constellation which is able to meet the mission requirements with a minimum number of spacecraft the algorithms discussed were demonstrated by designing a three spacecraft constellation which has access to the complete surface of the Moon during one orbital period. The results indicated the successful performance of the algorithms discussed in the current work. The practicality of this optimal constellation was studied by examining the antenna sizes and data transfer rate at the ground, which suggested that such a constellation could be achieved with existing small satellite technology.

Table 4. Performance and requirements of the communication system achieved through the designed constellation.

Parameter	Transmission to the Earth	Transmission to the Moon
Maximum beamwidth	2.25 deg	7.71 deg
Maximum range	438040 km	88107 km
Size of the antenna	**1.1 m**	**0.32 m**
Transmission gain	37.2 dB	26.5 dB
Power received	7×10^{-12} W	
Estimated bit rate	**1.14 Gbps**	

Future work on lunar constellation design will aim to improve the multidisciplinary nature of the problem. Aspects such as the fuel cost to deploy the spacecraft in the halo orbits starting from Earth, and station keeping fuel requirements will be factored into the design. Additionally, future work will also aim to include spacecraft level constraints such as mass, volume, and cost into the design. Such inclusions will enable the IDEAS framework to develop a holistic lunar relay constellation mission, thus progressing towards an end-to-end mission design solution.

REFERENCES

[1] Taylor, L.A., 1992, February. Return to the Moon: Lunar robotic science missions. In *Lunar Materials Technology*.

[2] Mendell, W.W., 1991. Lunar base as a precursor to Mars exploration and settlement. *Moon*, *110*(6), p.660.

[3] Crawford, I.A., Anand, M., Cockell, C.S., Falcke, H., Green, D.A., Jaumann, R. and Wieczorek, M.A., 2012. Back to the Moon: the scientific rationale for resuming lunar surface exploration. *Planetary and Space Science*, *74*(1), pp.3-14.

[4] Spann, J.F., Taylor, G.J. and Neal, C.R., 2008, July. Exploring the Moon in the 21st Century: Themes, Goals Objectives, Investigations, and Priorities, 2008: Theme 1, Goal 1c: Use the Moon as a Platform for Astrophysical, Heliophysical, and Earth-observing Studies. In *NLSI Lunar Science Conference* (Vol. 1415).

[5] Land, P., 1985. Lunar base design. In *Lunar bases and space activities of the 21st century* (p. 363).

[6] Duke, M.B., Mendell, W.W. and Roberts, B.B., 1985. Strategies for a permanent lunar base. In *Lunar bases and space activities of the 21st century* (p. 57).

[7] Zacny, K., Mungas, G., Mungas, C., Fisher, D. and Hedlund, M., 2008. Pneumatic excavator and regolith transport system for lunar ISRU and construction. In *AIAA SPACE 2008 conference & exposition* (p. 7824).

[8] Mueller, R.P. and King, R.H., 2008, January. Trade study of excavation tools and equipment for lunar outpost development and ISRU. In *AIP conference proceedings* (Vol. 969, No. 1, pp. 237-244). AIP.

[9] Nallapu, R., Thoesen, A., Garvie, L., Asphaug, E. and Thangavelautham, J., 2016. Optimized bucket wheel design for asteroid excavation. In *Proceedings of the International Astronautical Congress, IAC*. International Astronautical Federation, IAF.

[10] Thangavelautham, J., Smith, A., Abu El Samid, N., Ho, A., Boucher, D., Richard, J. and D'Eleuterio, G.M., 2008, January. Multirobot Lunar Excavation and ISRU Using Artificial-Neural-Tissue Controllers. In *AIP Conference Proceedings* (Vol. 969, No. 1, pp. 229-236). AIP.

[11] Novara, M., Putz, P., Maréchal, L. and Losito, S., 1998. Robotics for lunar surface exploration. *Robotics and autonomous systems*, *23*(1-2), pp.53-63.

[12] Brooks, R.A., Maes, P., Mataric, M.J. and More, G., 1990, July. Lunar base construction robots. In *EEE International Workshop on Intelligent Robots and Systems, Towards a New Frontier of Applications* (pp. 389-392). IEEE.

[13] Salisbury, F.B., 1991. Biogenerative life-support system: Farming on the Moon. *Acta astronautica*, *23*, pp.263-270.

[14] Klaus, D.M., Adams, A.C., Bamsey, M., Cragg, M., Ellis, T., Higgins, C.D., Howard, H.N., Jairala, J., Kelly, E.A., Krauser, W.R. and McFarland, S.M., 2005. *Spacecraft life support system design guidelines for human exploration of the Moon and Mars* (No. 2005-01-3008). SAE Technical Paper.

[15] Folta, D. and Quinn, D., 2006, August. Lunar frozen orbits. In *AIAA/AAS Astrodynamics Specialist Conference and Exhibit* (p. 6749).

[16] Beckman, M. and Lamb, R., 2007. Stationkeeping for the Lunar Reconnaissance Orbiter (LRO).

[17] Nallapu, R., and Thangavelautham, J., 2019, March. Attitude Control of Spacecraft Swarms for Visual Mapping of Planetary Bodies. In *2019 IEEE Aerospace Conference* (pp. 1-16). IEEE.

[18] Vallado, D.A, 2013. Fundamentals of Astrodynamics and Applications, Fourth Edition, *Space Technology Library.*

[19] Bate, R.R., Mueller, D.D. and White, J.E., 1971. *Fundamentals of astrodynamics*. Courier Corporation.

[20] Poincaré, H., 1992. *New methods of celestial mechanics* (Vol. 13). Springer Science & Business Media.

[21] Farquhar, R., 1968. The Control and Use of Libration-Point Satellites. *Ph.D. Thesis, Stanford University*.

[22] Zagouras, C.G. and Kazantzis, P.G., 1979. Three-dimensional periodic oscillations generating from plane periodic ones around the collinear Lagrangian points. *Astrophysics and Space Science*, *61*(2), pp.389-409.

[23] Howell, K.C. and Pernicka, H.J., 1987. Numerical determination of Lissajous trajectories in the restricted three-body problem. *Celestial Mechanics*, *41*(1-4), pp.107-124.

[24] Howell, K.C., 1984. Three-dimensional, periodic, 'halo orbits. *Celestial mechanics*, *32*(1), pp.53-71.

[25] Parker, J. and Hamera, K.E., 2007. Chaining Periodic Three-Body Orbits.

[26] Richardson, D.L. and Cary, N.D., 1975, July. A uniformly valid solution for motion about the interior libration point of the perturbed elliptic-restricted problem. In the *AIAA Conference on the Exploration of the Outer Planets*.

[27] Grebow, D., 2006. Generating periodic orbits in the circular restricted three-body problem with applications to

lunar south pole coverage. *MSAA Thesis, School of Aeronautics and Astronautics, Purdue University*.
[28] Anthony, W., Larsen, A. and Butcher, E., 2013. Optimal impulsive manifold-based transfers with guidance to Earth-Moon L1 halo orbits. In *23rd AAS/AIAA Space Flight Mechanics Meeting, Spaceflight Mechanics 2013* (pp. 2093-2112). Univelt Inc.
[29] Davis, K., Parker, J. and Butcher, E., 2015. Transfers from Earth to Earth-Moon L3 halo orbits using accelerated manifolds. *Advances in Space Research*, *55*(7), pp.1868-1877.
[30] Simó, C., Gómez, G., Llibre, J., Martinez, R. and Rodriguez, J., 1987. On the optimal station-keeping control of halo orbits. *Acta Astronautica*, *15*(6-7), pp.391-397.
[31] Williams, K., Wilson, R., Lo, M., Howell, K. and Barden, B., 2000. Genesis halo orbit station keeping the design.
[32] Farquhar, R.W., 1967. Lunar communications with libration-point satellites. *Journal of Spacecraft and Rockets*, *4*(10), pp.1383-1384.
[33] Ely, T.A. and Lieb, E., 2006. Constellations of elliptical inclined lunar orbits providing polar and global coverage. *the Journal of the Astronautical Sciences*, *54*(1), pp.53-67.
[34] Circi, C., Romagnoli, D. and Fumenti, F., 2014. Halo orbit dynamics and properties for a lunar global positioning system design. *Monthly Notices of the Royal Astronomical Society*, *442*(4), pp.3511-3527.
[35] Hamera, K., Mosher, T., Gefreh, M., Slavkin, L., Paul, R. and Trojan, J., 2008, June. An Evolvable Lunar Communication and Navigation Constellation Architecture. In *26th International Communications Satellite Systems Conference (ICSSC)*.
[36] Wertz, J.R., Everett, D.F. and Puschell, J.J., 2011. *Space mission engineering: the new SMAD*. Microcosm Press.
[37] Nallapu, R., and Thangavelautham, J., "Spacecraft Swarm Attitude Control for Small Body Surface Observation," *In 2019 Advances in the Astronautical Sciences (AAS) GNC Conference Proceedings*, AAS-GNC, 2019.
[38] Nallapu, R., Thangavelautham, J., "*Towards End-To-End Design of Spacecraft Swarms for Small-Body Reconnaissance*," Proceedings of the 70th International Astronautical Congress, IAF, Washington D.C.
[39] Nallapu, R., and Thangavelautham, J., "Cooperative Multi-spacecraft Observation of Incoming Space Threats", 2019 Advanced Maui Optical Science (AMOS) Proceedings, AMOS Tech.,2019.
[40] 3D Asteroid Catalogue. 2013, https://3d-asteroids.space/moons/E1-Moon , (accessed 10.15.2019)
[41] Conn, A.R., Gould, N.I. and Toint, P., 1991. A globally convergent augmented Lagrangian algorithm for optimization with general constraints and simple bounds. *SIAM Journal on Numerical Analysis*, *28*(2), pp.545-572.
[42] Kobayashi, M., 2017. Iris Deep-Space Transponder for SLS EM-1 CubeSat Missions.
[43] Taylor, J., 2016. The Deep Space Network: A Functional Description. *Deep Space Communications*, pp.15-35.

BIOGRAPHY

Ravi teja Nallapu *received his B.Tech. in Mechatronics Engineering from JNTU, India in 2010, and an M.S in Aerospace Engineering from the University of Houston, TX in 2012. He then worked with U.S Airways as a Flight Simulator Engineer for 2 years. He is presently pursuing his Ph.D. in Aerospace Engineering at SpaceTREx Laboratory at the University of Arizona, Az. His research interests include GNC of spacecraft swarms, dynamics around small bodies, interplanetary trajectory design, and attitude control.*

Leonard D. Vance *is a Ph.D. candidate in Aerospace and Mechanical Engineering at the University of Arizona. He is a retired senior fellow with 34 years of mostly space and space-related experience at Hughes Aircraft Company, later becoming part of the Raytheon Corporation. Areas of expertise include simulations, guidance and control, and preliminary systems design. Fields of study emphasize the exploitation of small spacecraft for Earth and planetary exploration.*

Jekan Thangavelautham *is an Assistant Professor and has a background in aerospace engineering from the University of Toronto. He worked on Canadarm, Canadarm 2 and the DARPA Orbital Express missions at MDA Space Missions. Jekan obtained his Ph.D. in space robotics at the University of Toronto Institute for Aerospace Studies (UTIAS) and did his postdoctoral training at MIT's Field and Space Robotics Laboratory (FSRL). Jekan Thanga heads the Space and Terrestrial Robotic Exploration (SpaceTREx) Laboratory at the University of Arizona. He is the Engineering Principal Investigator on the AOSAT I CubeSat Centrifuge mission and is a Co-Investigator on SWIMSat, an Airforce CubeSat mission to monitor space threats.*